Surface tension and size effect in ferroelectric nanotubes

2008 J. Phys.: Condens. Matter 20 135216

(http://iopscience.iop.org/0953-8984/20/13/135216)

J. Phys.: Condens. Matter **20** (2008) 135216 (9pp) doi:10.1088/0953-8984/20/13/135216

Surface tension and size effect in ferroelectric nanotubes

Yue Zheng[1,2], C H Woo[1] and Biao Wang[3]

[1] Department of Electronic and Information Engineering, The Hong Kong Polytechnic University, Hong Kong SAR, People's Republic of China
[2] Electro-Optics Technology Center, Harbin Institute of Technology, Harbin 150001, People's Republic of China
[3] State and Key Laboratory of Optoelectronic Materials and Technologies, Institute of Optoelectronic and Functional Composite Materials and School of Physics and Engineering, Sun Yat-sen University, Guangzhou, People's Republic of China

E-mail: yuezheng@hit.edu.cn and chung.woo@polyu.edu.hk

Received 4 November 2007, in final form 19 February 2008
Published 12 March 2008
Online at stacks.iop.org/JPhysCM/20/135216

Abstract
Using a thermodynamic model, linear stability analysis is performed on the associated dynamic Ginsburg–Landau equation for a ferroelectric nanotube. Analytic expressions of the transition temperature and Curie–Weiss relation are derived. The ferroelectric properties of the tube are found to generally depend on its dimensions through effects of the surface tension and near-surface eigenstrain relaxation. Our results also show that the transition temperature and polarization are both enhanced due to the dominance of the effective radial pressures induced by the surface tension, resulting in a remnant polarization and coercive field that may become larger than the bulk values.

(Some figures in this article are in colour only in the electronic version)

1. Introduction

Research on ferroelectric nanostructures is experiencing a rapid surge of interest due to their potential usefulness in applications such as nanoscale piezoelectric transducers, electro-optic devices, nonvolatile memory devices, etc. Theory and experiments on ferroelectric thin films (TFs), nanoparticles (NPs), nanowires (NWs), nanorods (NRs), nanodisks (NDs) and nanotubes (NTs) all indicate strong surface effects on their polarization [1–16]. This is expected because the large surface to volume ratio in such cases naturally leads to strong surface effects. Indeed, the tendency to minimize the surface energy introduces a large intrinsic surface stress, i.e. surface tension, in samples of nanodimension, and is one of the most important surface effects considered. The role of surface tension may be seen from the significant polarization enhancement of PBST ($Pb_{0.25}Ba_{0.15}Sr_{0.6}TiO_3$) in nanotube form compared with that in thin-film form [1]. In another case, a giant reversible piezoelectric strain in a 70 nm diameter $PbZr_{0.2}Ti_{0.8}O_3$ NW was observed [6] in the presence of a large compressive stress due to the surface tension. In ultra-small $PbZr_{0.52}Ti_{0.48}O_3$ NRs and NTs with radii R between 20 and 30 nm and length 50 μm, a rectangular shaped piezoelectric hysteresis loop was observed with an effective remnant piezoelectric coefficient comparable with that typically found in PZT films. By using x-ray diffraction (XRD), Uchino *et al* [12] investigated the effect of particle size on the Curie temperature of $BaTiO_3$. The abrupt change of the Curie temperature with the observed particle size was found to corroborate the large compressive pressure induced by the surface tension. Theoretically, Huang *et al* [10, 11] considered the effect of bond contraction on the surface layers of NPs, which induces a compressive stress on the inner part. The phase transition and other ferroelectric properties of NPs are also found to be size dependent.

The proximity of the surface is also known to affect the polarization of a ferroelectric sample. Indeed, since the polarization is derived from the eigenstrain (transformation strain) associated with the structural instability of the crystal lattice, it naturally varies according to the atomistic environment of the location under consideration. The large disruption of crystalline uniformity near the surface is expected to affect the eigenstrain and hence the polarization. This effect of surface relaxation on the spontaneous polarization has been modeled using an

extrapolating length by many of the theoretical investigations of the ferroelectric properties of the TFs, NPs, NWs and NRs based on the Landau phenomenological theory. Thus, Zhong *et al* [9] investigated the size effect on the Curie temperature and polarization of a spherical NP and found a diminishing polarization and Curie temperature as the extrapolation length decreases. Using the direct variational method [13, 14], an approximate analytical expression for the paraelectric–ferroelectric transition temperatures for NRs and NWs has been derived as a function of size, extrapolation length and effective surface tension. Using first-principle calculations, Fu *et al* [8] investigated the polarization and Curie temperature of one-dimensional ferroelectric NWs and found that the polarization and Curie temperature of NWs was size dependent, and that ferroelectricity disappeared completely when the radius of the NW was reduced below a critical value.

Both effects alter the free energy of a bulk ferroelectric, causing the phase transition temperature to shift and polarization to change [13, 15]. This forms the subject of the present study. In the following, using a thermodynamic model and linear stability analysis of the associated dynamic equation, analytic expressions of the transition temperature and Curie–Weiss relation of ferroelectric NTs are derived and analyzed, paying particular attention to the effects of the surface tension and surface relaxation. We shall consider the transition temperature and Curie–Weiss relation as a function of tube dimensions through the actions of the surface tension, polarization gradient coefficient, extrapolation length, and electrostriction coefficient. The implications of the results will be considered and discussed.

2. Formulation

2.1. The system free energy

As in our previous calculations, the order parameter we use to describe the transition between the paraelectric and ferroelectric phases is the self-polarization [16–18] $\mathbf{P} = (0, 0, P)$. $\mathbf{P}$ is the result of the permanent atomic displacements responsible for the spontaneous polarization generated when a crystal becomes unstable, for example going through a phase transformation. It is a function of the sample temperature, as well as other variables such as electric field and mechanical stresses. In the absence of the external field and depolarization field, $\mathbf{P}$ is the spontaneous polarization of an infinite crystal, which we use as our reference state. At stable equilibrium positions, i.e. far from unstable atomic configurations, an electric field $\mathbf{E}$ can also induce a polarization $\mathbf{P}^E$ proportion to $\mathbf{E}$ via small non-permanent atomic displacements that vanishes upon the removal of $\mathbf{E}$. The directly measurable polarization $\mathbf{P}^{\mathrm{T}}$ can be written as the sum of $\mathbf{P}$ and $\mathbf{P}^E$. Since small atomic displacements are involved, $\mathbf{P}^E$ may be assumed to be linearly proportional to $\mathbf{E}$ with a constant susceptibility $\boldsymbol{\chi}_{\mathrm{d}}$ that is characteristic of the current phase of the background material [15–21]. The electric displacement is then given by

$$\begin{aligned}\mathbf{D} &= \boldsymbol{\varepsilon}_0\mathbf{E} + \mathbf{P}^{\mathrm{T}} = \boldsymbol{\varepsilon}_0\mathbf{E} + \mathbf{P}^{\mathrm{E}} + \mathbf{P} \\ &= \boldsymbol{\varepsilon}_0\mathbf{E} + \boldsymbol{\chi}_{\mathbf{d}}\mathbf{E} + \mathbf{P} = \boldsymbol{\varepsilon}_{\mathbf{d}}\mathbf{E} + \mathbf{P},\end{aligned} \tag{1}$$

where $\boldsymbol{\varepsilon}_0$ are dielectric constants of the vacuum. $\boldsymbol{\varepsilon}_{\mathrm{d}}$ is the dielectric constant of the current phase of the background material. When we consider the effect of the depolarization field, $\mathbf{E}$ is the sum of the external electric field $\mathbf{E}_{\mathrm{ext}}$ and the depolarization field $\mathbf{E}_{\mathrm{d}}$. Indeed, in the absence of an external electric field, the total electric field has only one contribution, that is the depolarization field $\mathbf{E}_{\mathrm{d}}$, i.e. $\mathbf{E} = \mathbf{E}_{\mathrm{d}}$, and the electric displacement is given by

$$\begin{aligned}\mathbf{D} &= \boldsymbol{\varepsilon}_0\mathbf{E}_{\mathrm{d}} + \mathbf{P}^{\mathrm{T}} = \boldsymbol{\varepsilon}_0\mathbf{E}_{\mathrm{d}} + \mathbf{P}^{\mathrm{E}} + \mathbf{P} \\ &= \boldsymbol{\varepsilon}_0\mathbf{E}_{\mathrm{d}} + \boldsymbol{\chi}_{\mathrm{d}}\mathbf{E}_{\mathrm{d}} + \mathbf{P} = \boldsymbol{\varepsilon}_{\mathrm{d}}\mathbf{E}_{\mathrm{d}} + \mathbf{P}.\end{aligned} \tag{2}$$

In the following, we consider the simplified one-dimensional case where all vector fields are directed in the z-direction and susceptibilities and permittivities are diagonal, so that all vectors in the foregoing can be represented by their magnitudes. In general, the polarization does not necessarily concentrate along the z direction, and the radial components should be considered. In our paper, however, we are mainly concerned in a qualitative sense with effects caused by the large surface to volume ratio in a ferroelectric nanotube, and the physical reasons behind them. In such cases, a reasonable simplifying assumption of the polarization directions relative to the specimen geometry may be justifiable, particularly in view of the complications in the formulation and computation, which can be avoided. Indeed, under short-circuit electric boundary conditions, under the effective radial pressures due to the surface tension, the polarization is easily aligned along the z direction [13].

Based on Landau–Ginzburg–Devonshire (LGD) theory, the total free energy of a ferroelectric can be expressed as

$$F = F_{\mathrm{bulk}} + F_{\mathrm{grad}} + F_{\mathrm{Ele}} + F_{\mathrm{s}}, \tag{3}$$

where F_{bulk}, F_{grad}, F_{Ele} and F_{s} are the bulk energy, gradient energy, electric field and surface energy, respectively.

The free energy density expansion on the order parameter P for a field-free (i.e. $E = 0$ and $P^E = 0$) infinite ferroelectric under mechanical stresses σ_{ij} is given by

$$\begin{aligned}f_{\mathrm{bulk}} = {} & \frac{\alpha_0}{2}(T - T_{\mathrm{c0}})P^2 + \frac{\beta}{4}P^4 + \frac{\gamma}{6}P^6 \\ & - Q_{12}(\sigma_{11} + \sigma_{22})P^2 - Q_{11}\sigma_{33}P^2 - f(\sigma_{ij}),\end{aligned} \tag{4}$$

where α_0, β and γ are the expansion coefficients of the Landau free energy. T_{c0} is the Curie–Weiss temperature of the bulk material, Q_{ij} the electrostriction tensor and $f(\sigma_{ij}) = \frac{1}{2}s_{ijkl}\sigma_{ij}\sigma_{kl}$ a function of only external stresses [22].

In the following, we consider the specific case of a ferroelectric NT with inner radius a, outer radius b, average radius $R = (a + b)/2$, length h and wall thickness w as shown in figures 1(b) and (c). We use a cylindrical co-ordinate system in which the major component of the polarization is along the z direction.

The surface tension creates a radial compression of the NT. The first term F_{bulk} of equation (3) in cylindrical coordinates (r, φ, z) then becomes

$$\begin{aligned}F_p = 2\pi \int_{-h/2}^{h/2} \mathrm{d}z \int_a^b r\,\mathrm{d}r \Bigg\{ & \frac{\alpha_\sigma}{2}P^2(r, z) + \frac{\beta}{4}P^4(r, z) \\ & + \frac{\gamma}{6}P^6(r, z) - f(\sigma_{ij})\Bigg\}.\end{aligned} \tag{5}$$

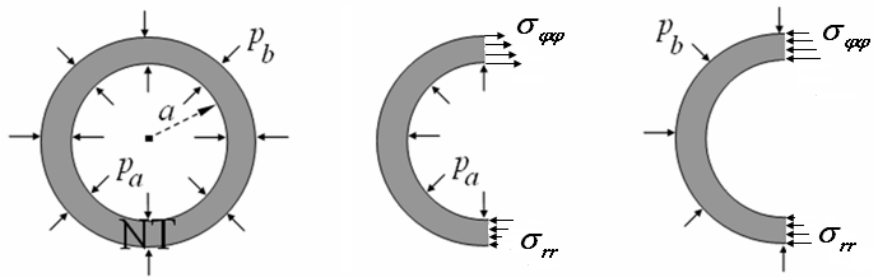

Figure 1. Schematic diagrams of the stress field in the thick-wall tube problem under applied inner and outer radial pressures.

The expression of α_σ is given by [13, 23]

$$\alpha_\sigma = \alpha_0(T - T_{c0}) - 2Q_{12}(\sigma_{rr} + \sigma_{\varphi\varphi}) - Q_{11}\sigma_{zz}, \quad (6)$$

where σ_{rr} and $\sigma_{\varphi\varphi}$ are the radial and tangential components of the stress field in the NT induced by the surface tension. These will be furthered discussed in the next section.

The Ginzburg gradient term F_{grad} in the free energy expression equation (3) becomes significant in the nanoscale and must be included in our present calculation, where it can be written as [13, 14, 24]

$$F_{\text{grad}} = 2\pi \int_{-h/2}^{h/2} \mathrm{d}z \int_a^b r\mathrm{d}r \left\{ \frac{D}{2} [\nabla P\,(r,z)]^2 \right\}, \quad (7)$$

D can be approximated as $\xi^2|\alpha(T - T_{c0})|$, where ξ is a characteristic length along which the polarization varies.

In the absence of an external electric field, the third term of equation (3) accounts for the electric energy due to the depolarization field E_{d} along the z direction. The third term should be expressed as [16]

$$F_{\text{Ele}} = 2\pi \int_{-h/2}^{h/2} \mathrm{d}z \int_a^b r\,\mathrm{d}r \left\{ -\tfrac{1}{2} E_{\text{d}} P^T(r,z) \right\}. \quad (8)$$

In the present study, we only consider the short-circuit boundary condition, which can be derived by solving the electrostatic equilibrium, such as for an NW in [13]. Nevertheless, we may assume that the depolarization field along z direction can be neglected because the NT is long. So the polarization P^E induced by the depolarization field can be neglected.

The last term F_{s} of equation (3) accounts for surface contributions to the total free energy. Taking into account contributions from the top, bottom and sidewalls, F_{s} can be expressed as [13, 23]

$$\begin{aligned} F_{\text{s}} = {} & D \int_a^b \frac{2\pi r}{\delta_{\text{end}}} \left[P^2(r, z = h/2) + P^2(r, z = -h/2) \right] \mathrm{d}r \\ & + D \int_{-h/2}^{h/2} \frac{2\pi a}{\delta} P^2(r = a, z)\,\mathrm{d}z \\ & + D \int_{-h/2}^{h/2} \frac{2\pi b}{\delta} P^2(r = b, z)\,\mathrm{d}z, \end{aligned} \quad (9)$$

where δ_{end} and δ are the extrapolation lengths at the end surfaces and the sidewall of the nanotube, respectively. As discussed, the extrapolation length takes into account surface effects on the polarization. Two separate cases may be considered: (i) the more common case $\delta > 0$, which corresponds to a reduction of polarization near the surface; and (ii) the rarer case $\delta < 0$, corresponding to an enhancement. We note that in general δ is not a constant, and should be determined experimentally or by first-principle calculations for different ferroelectric materials and boundary conditions [24, 25].

2.2. Surface tension in nanoscale ferroelectric tube

Nanocrystals generally have a large surface to volume ratio. The tendency to minimize the surface energy density is often sufficiently large to significantly affect the properties of the nanocrystal. Experimentally, Ma *et al* [5] and Uchino *et al* [12] noted that the effects of surface tension on a nanocrystal are analogous to a hydrostatic pressure on a bulk single crystal.

For ferroelectric NWs, NRs or NPs, surface effects expressed in terms of the extrapolation length can change the polarization near surfaces and associated properties. At the same time, the surface tension produces a radial pressure, which is expected to affect properties such as Curie temperature, polarization and dielectric constant, etc, similar to an effective radial compression. Based on the Landau–Devonshire equation, Huang *et al* [10, 11] investigated the effect of grain size on ferroelectric nanoparticles in solid solution. They considered a compressive stress inside a ferroelectric spherical particle caused by surface bond contraction. Morozovska *et al* [13, 26] found that the surface tension in finite-size NRs/NWs/NDs played a role similar to an epitaxial stress in thin films. The uniform radial stress due to the surface tension μ/R in an NR, with surface energy density μ and radius R, compresses the NR in the transverse direction and stretches it along the polar axis z. Recently, Zhou *et al* [6] also illustrated the effect of the surface tension and internal compressive stress on the properties of ferroelectric NWs. By a similar reasoning, surface tension in a ferroelectric NT should also experience similar effects.

The linear elastic problem of a thick-wall tube under radial pressures p_a and p_b at the inner and outer surfaces (see figure 1) has been solved by Lame [27]. The resulting stress field can be expressed in cylindrical coordinates (r, φ, z) as

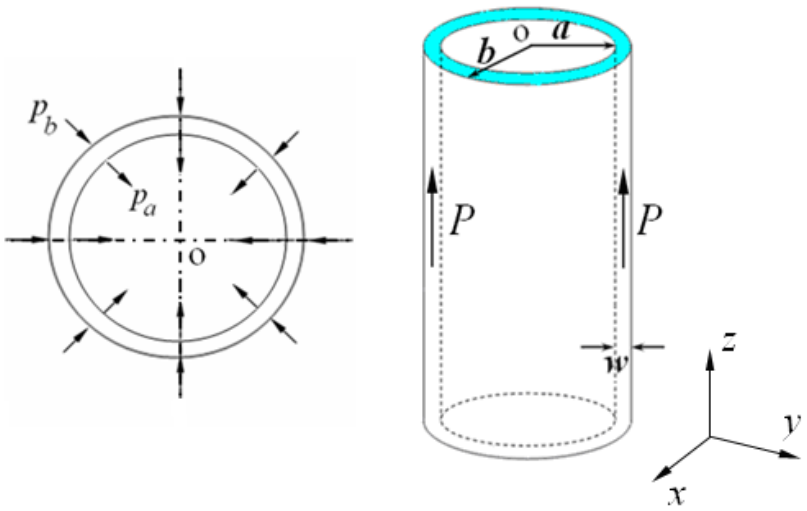

Figure 2. Schematic diagrams of an NT under the effective radial pressures $p_a = -\mu_a/a$ and $p_b = \mu_b/b$ induced by the surface tension.

follows:

$$\sigma_{rr}(r) = \frac{a^2}{b^2-a^2}\left(1-\frac{b^2}{r^2}\right)p_a - \frac{b^2}{b^2-a^2}\left(1-\frac{a^2}{r^2}\right)p_b,$$
$$\sigma_{\varphi\varphi}(r) = \frac{a^2}{b^2-a^2}\left(1+\frac{b^2}{r^2}\right)p_a - \frac{b^2}{b^2-a^2}\left(1+\frac{a^2}{r^2}\right)p_b,$$
$$\sigma_{r\varphi} = 0, \quad \sigma_{rz} = 0, \quad \sigma_{zz} = 0, \quad \sigma_{z\varphi} = 0, \tag{10}$$

For the NT, the radial stresses p_a and p_b in equation (10) can be approximately expressed in terms of the surface energy densities μ_a and μ_b, i.e. $p_a = -\mu_a/a$ and $p_b = \mu_b/b$ (see figure 2) [28]. We note that when the inner radius a of the NT is zero, equation (10) reduces to the stress field of an NR (i.e. $a = 0$ and $b = R$), which has been discussed in [13, 14].

From equations (5) and (9), the normalized coefficient $\alpha_\sigma(T)$ can be rewritten in terms of the surface tension $\sigma_{\rm st}$,

$$\alpha_\sigma = \alpha_0(T - T_{c0}) - 2Q_{12}\sigma_{\rm st}, \tag{11}$$

where $\sigma_{\rm st}$ is a function of the inner and outer radii, and can be expressed as

$$\sigma_{\rm st} = \sigma_{rr} + \sigma_{\varphi\varphi} = \frac{a^2}{b^2-a^2}p_a - \frac{b^2}{b^2-a^2}p_b$$
$$= -\frac{a\mu_a + b\mu_b}{b^2-a^2} = -\frac{\bar{\mu}}{w} - \frac{\Delta\mu}{2R}, \tag{12}$$

where $\bar{\mu}$ is the average surface energy density and $\Delta\mu = (\mu_b - \mu_a)/2$. The minus sign in equation (12) indicates a compression. We also note that equation (12) is inapplicable when $b \approx a$ because the magnitude of the stresses would have exceeded the validity of elasticity theory, and plastic yielding would have occurred. Assuming a simple elastic–plastic model with a yield stress $\sigma_{\rm Y}$, we may rewrite $\alpha_\sigma(T)$ in the form [29, 30]

$$\alpha_\sigma(T, a, b) = \alpha_0(T - T_{c0}) - 2Q_{12}\sigma_{\rm st}^{\rm eff}, \tag{13}$$

with an effective stress due to the surface tension defined as

$$\sigma_{\rm st}^{\rm eff} = \begin{cases} -\dfrac{\bar{\mu}}{w}\left(1 + \dfrac{w\Delta\mu}{2R\bar{\mu}}\right) & \text{for } w > w_Y \\ -\sigma_Y & \text{for } w \leqslant w_Y, \end{cases} \tag{14}$$

where w_Y is the thickness below which plastic yield occurs. Of course, we can construct an approximated function based on equation (14) to fit the effective stress, which can be given by $\sigma_{\rm st}^{\rm eff} = -\sigma_{\rm Y}[1 - \exp(-w_{\rm Y}/w)]$. The use of $\sigma_{\rm st}^{\rm eff}$ helps us avoid the unphysical divergence at $b \approx a$. We note that if $|\frac{w\Delta\mu}{2R\bar{\mu}}| \ll 1$, which is usually satisfied, $\sigma_{\rm st}^{\rm eff}$ is independent of the average tube radius R, and any size dependence of the ferroelectric properties of the tube is dominated by the wall thickness and the extrapolation length. We note that effects on the polarization due to the strain fields on the dislocations generated at the yield may be important, but is a complicated problem that has to be considered as an issue on its own.

2.3. Phase transition temperature, Curie–Weiss relation and polarization

The time evolution of the system is governed by the time-dependent Ginzburg–Landau (TDGL) equation [7, 8]. Using equations (3) and (13), this can be written as

$$\frac{\partial P}{\partial t} = -M\frac{\delta F}{\delta P} = -M\left\{\alpha_\sigma(T, r)P(r) + \beta P^3(r) + \gamma P^5(r) - D\frac{1}{r}\frac{\partial}{\partial r}\left(r\frac{\partial P(r)}{\partial r}\right)\right\}, \tag{15}$$

where M is the kinetic coefficient related to the domain wall mobility, and $\delta F/\delta P$ is the thermodynamic force driving the spatial and temporal evolution. We note that in equation (15) the depolarization field has been neglected because of the long ferroelectric NT being only considered in this section.

The surface term in equation (9) yields the boundary conditions [13, 17]

$$\frac{\partial P}{\partial r} = \frac{P}{\delta}, \qquad \text{for } r = a, \qquad \text{and}$$
$$\frac{\partial P}{\partial r} = -\frac{P}{\delta}, \qquad \text{for } r = b. \tag{16}$$

Equation (15) has a trivial solution $P = 0$, representing the stationary paraelectric state. To be able to transform between the paraelectric ($P = 0$) and the ferroelectric ($P \neq 0$) states, the initial state must become dynamically unstable. The dynamical stability of the initial state can be probed by applying a small perturbation Δ to the corresponding stationary solution of equation (15). The dynamics of Δ follows from equation (15) by retaining only terms linear in Δ, which is given by

$$\frac{\partial \Delta}{\partial t} = -M\left[\alpha_\sigma \Delta + 3\beta P^3 \Delta + 6\gamma P^5 \Delta - D\frac{1}{r}\frac{\partial}{\partial r}\left(r\frac{\partial \Delta}{\partial r}\right)\right]. \tag{17}$$

In the general case equation (17) must be solved by using the Bessel functions. For simplicity, we only approximately assume that the gradient term in the thin wall of NT is the same as it is in thin film [18]. The boundary condition is the same as equation (16), only with P replaced by Δ. For a symmetric configuration, the condition $\mathrm{d}\Delta/\mathrm{d}r = 0$, at $r = a + w/2$, must also hold.

Using the method of separation of variables, the TDGL equation can be transformed into an eigenvalue problem. For the $P = 0$ state, the solution can be written as $\Delta_c(r, t) = \mathrm{e}^{\omega_c t}\varphi_{\omega_c}(r)$, where ω_c is the eigenvalue, and $\varphi_{\omega_c}(z)$ the corresponding eigenfunction of equation (TDGL),

$$\omega_c = M[-\alpha_\sigma - Dk^2]. \tag{18}$$

The $P = 0$ stationary solution is unstable when $\omega_c > 0$, because in this case the perturbation Δ increases exponentially with time. It can be seen from equation (16) that when the temperature T is sufficiently high $\omega_c < 0$, and the paraelectric state is stable. When T is sufficiently low, ω_c turns positive and this state is no longer stable, since any small perturbation Δ will grow exponentially beyond all bounds. The critical condition, $\omega_c = 0$, yields, in this case, the transition temperature T_c of the film [15, 16, 28, 30],

$$T_c = T_{c0} + \frac{2Q_{12}}{\alpha_0}\sigma_{st}^{\text{eff}} - \frac{D}{\alpha_0}k_c^2, \tag{19}$$

where the first term on the RHS is related to the bulk ferroelectric property, the second term to the surface tension, and the third term to the lattice relaxation on the surface. While the last term acts against the transformation by lowering the transition temperature, the second term may act either way, depending on the effective radial pressures, i.e. p_a and p_b. Here k_c depends on the wall thickness w and the extrapolating length δ, as the smallest non-zero root of the transcendental equation [15, 18, 26, 29, 30],

$$\cot\left(\frac{k_c w}{2}\right) - k_c\delta = 0. \tag{20}$$

Analytic solutions of equation (20) have been obtained [15] in our previous calculations for various important limits and approximations. Thus, for thin-walled tubes, i.e. $w \ll \delta$, $k_c^2 = \frac{2}{w(\delta + w/6)}$, so that equation (19) can be written as

$$T_c = T_{c0} + \frac{2Q_{12}}{\alpha_0}\sigma_{st}^{\text{eff}} - \frac{2D}{\alpha_0 w(\delta + w/6)}. \tag{21}$$

The corresponding critical wall thickness for a positive T_c is given by

$$w_c \approx \frac{2D}{\delta(4Q_{12}\sigma_{st}^{\text{eff}} + \alpha_0 T_{c0})}. \tag{22}$$

When $w \gg \delta$, solution of equation (20) gives $k_c = \frac{\pi}{w + 2\delta}$ and equation (19) for the transition gives

$$T_c = T_{c0} + \frac{2Q_{12}}{\alpha_0}\sigma_{st}^{\text{eff}} - \frac{D}{\alpha_0}\left(\frac{\pi}{w + 2\delta}\right)^2. \tag{23}$$

Neglecting δ in comparison with w, the corresponding critical wall thickness for a positive T_c can be easily solved, and is given by

$$w_c \approx \sqrt{\frac{\pi^2 D}{(2Q_{12}\sigma_{st}^{\text{eff}} + \alpha_0 T_{c0})}}. \tag{24}$$

We note that in both limits of $w \ll \delta$ (small surface relaxation) and $w \gg \delta$ (large relaxation) the surface effect due to δ (the third term on the RHS) causes the transition temperature to decrease monotonically as the wall thickness w of the tube decreases, while the surface tension has the opposite effect, except when the wall thickness is below w_Y. As $w < 2R$ always holds, for $\frac{\Delta\mu}{\bar{\mu}} \ll 1$, σ_{st}^{eff} is independent of R and both T_c and w_c are independent of R.

The susceptibility χ can be expressed as a function of P via the total free energy density f_{total} of the NT,

$$\chi^{-1} = \left(\frac{\partial^2 f_{\text{total}}}{\partial P^2}\right) = \alpha_0 (T - T_c) + 3\beta P^2 + 5\gamma P^4, \tag{25}$$

where T_c is the phase transition temperature of the NT as given by equation (19). Using equation (25), a Curie–Weiss-type relation of the spatial average $\langle\chi\rangle$ of a ferroelectric NT near the Curie temperature can be expressed in the following form [18]:

$$\langle\chi\rangle = \begin{cases} \dfrac{\Theta^{-1}(\delta, w)}{\alpha_0 |T - T_c|} & \text{for } T < T_c, \\ \dfrac{1}{\alpha_0 |T - T_c|} & \text{for } T > T_c, \end{cases} \tag{26}$$

where $\Theta(\delta, w)$ is the Curie–Weiss parameter as a function of the extrapolation length and wall thickness of the tube. Based on our previous calculations in [18], an approximated equation of the Curie–Weiss parameter can be obtained.

It is also of interest to directly evaluate the strength of the polarization. In terms of the Curie–Weiss relation, the spatially averaged free energy density can be written as

$$\Delta F = \frac{\alpha_0}{2}(T - T_c)\bar{P}^2 + \frac{\beta}{4}\bar{P}^4 + \frac{\gamma}{6}\bar{P}^6 - f(\sigma_{ij}), \tag{27}$$

where T_c is the phase transition temperature of the tube from equation (19), as a function of its wall thickness, radius and extrapolation length. Here we note that $\bar{P}$ is a spatial average.

Using the variational method, free energy minimization with respect to $\bar{P}$ yields the following equation [13, 26–33]:

$$\alpha_0 [T - T_c(R, w, \delta)] \bar{P} + \beta \bar{P}^3 + \gamma \bar{P}^5 = 0, \qquad (28)$$

which must be satisfied by $\bar{P}$, yielding

$$\bar{P} = \left[\frac{-\beta \pm \sqrt{\beta^2 - 4\alpha_0 \gamma \left[T - T_c(R, w, \delta)_c\right]}}{2\gamma} \right]^{1/2}, \qquad (29)$$

as a function of the wall thickness, radius and extrapolation length of the ferroelectric NT.

2.4. Polarization switching

Many experiments indicate that the surface tension may produce a large enhancement of the ferroelectric properties of an NT, such as the remnant polarization and the coercive field [1, 2]. In the following, we study polarization switching and hysteresis loops in a ferroelectric NT by considering its response to a sinusoidal electric field applied along the z direction [19–23],

$$E_{ext} = E_0 \sin\left(\frac{2\pi t}{T_p}\right) = E_0 \sin(2\pi f' t). \qquad (30)$$

Here E_0, T_p and f' are the amplitude, period and circular frequency, respectively. From equation (15), the time evolution of the polarization can be calculated numerically from TDGL with this sinusoidal electric field. A finite-difference method for spatial derivatives and the Runge–Kutta method for temporal derivatives are employed [17–20]. We note that the effects of the induced polarization by the external electric field together with the corresponding electrostrictive stresses are also included. So the total polarization is the sum of the self-polarization and induced polarization of equation (1).

3. Results and discussions

The analytical and numerical calculations in this paper are for $BaTiO_3$ (BTO) nanotubes, which have been successfully fabricated and implemented in various devices, such as capacitor and nonvolatile memories etc [2, 4, 29]. We only consider the case of a long tube with length h much larger than its inner/outer radius, so that the depolarization field can be neglected [12, 13, 15], thus allowing us to concentrate on the effects of the surface tension.

3.1. The transition temperature, Curie–Weiss law, and polarization

We first consider, as in [5, 13, 19, 34], the ideal case where the difference between the surface energy densities of the inner and outer surfaces is negligible, i.e. $\Delta\mu \approx 0$. Since typical values of the effective surface tension coefficient vary between 5 and 50 N m^{-1} [5, 13], we use a value of $\mu_a = \mu_b = \mu = 20$ N m^{-1}. Other material constants, such as the electrostrictive coefficients, the extrapolation length and the elastic properties, are from the literature [9, 16, 19, 22, 28, 35].

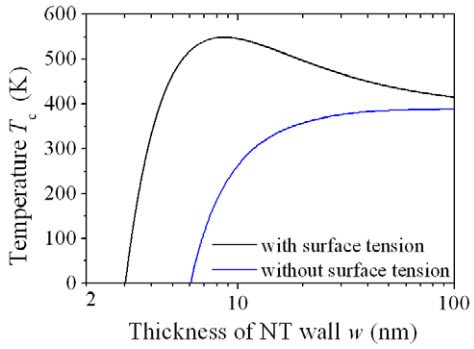

Figure 3. The phase transition temperature T_c versus the wall thickness w of an NT, where the inner radius is $a = 10$ nm, considering the surface tension effect (black line) and without considering the surface tension effect (blue line).

Phase transition temperatures T_c are calculated for various wall thicknesses w of an NT with inner radius $a = 10$ nm by solving equations (19) and (20). The results are plotted in figure 3, as a function of w. The important feature that can immediately be discerned is the maximum shown by T_c at $T_c^{max} \approx 580$ K for a wall thickness of $w \approx 8.5$ nm. Furthermore, for wall thickness larger than ~4 nm, T_c is actually higher than that of the bulk material at 400 K.

For comparison, the calculation was repeated without the surface tension contributions, i.e. by setting $\mu = 0$ N m^{-1}, and plotted as the blue line in figure 3. It can be seen from the comparison that the surface tension is responsible for the rise of the transition temperature, with a magnitude that tends to increase with the increasing surface tension as w decreases. As the compression due to the surface tension stops increasing beyond the elastic limit, the effects of the near-surface eigenstrain relaxation described by the extrapolation length δ starts to dominate and lower the transition temperature as w decreases (see equations (21) and (23)). As a result, the rise in T_c shows a maximum of $T_c^{max} \approx 580$ K at a wall thickness of $w \approx 8.5$ nm. According to these results, in addition to materials constants such as the Landau free energy parameters, the surface energy density and extrapolation length, the transition temperature of the NT is also sensitive to geometry parameters such as the wall thickness w.

In comparison with thin films, the operation of the surface tension leads to the following important differences: (1) in contrast to thin films in which the transition temperature monotonically decreases with decreasing film thickness, the transition temperature for NTs attains a maximum as the wall thickness decreases, and (2) the critical thickness for the disappearance of ferroelectricity in an NT is significantly larger than that of the thin film, and sometimes even the bulk material. Similar observations for ferroelectric NWs and thin films have been discussed in [13, 14, 16, 28].

In pure materials, the surface energy densities between the inner and outer wall surfaces of the NT are the same, so that it is reasonable to assume that $\Delta\mu \approx 0$. However, practical considerations sometimes require this condition to be relaxed, such as in cases where the environments encountered

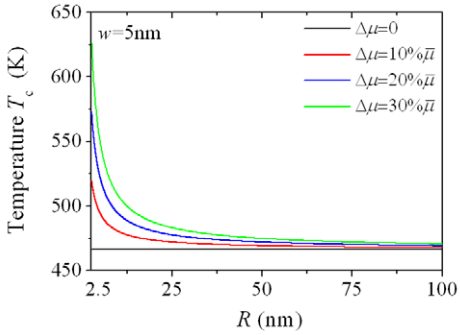

Figure 4. The phase transition temperature T_c versus the average radius R, where the inner and outer surface tension coefficient is considered as a difference, such as $\Delta\mu = 10\%\bar{\mu}$, $20\%\bar{\mu}$ and $30\%\bar{\mu}$.

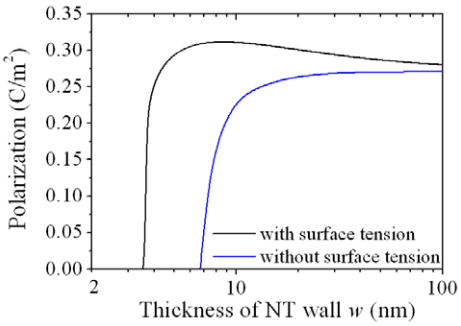

Figure 5. The polarization versus the wall thickness of NT at room temperature, where the inner radius is $a = 10$ nm, considering the surface tension effect (black line) and without considering the surface tension effect (blue line).

by the inner and outer surfaces are different. We consider that properties of ferroelectric NTs can be changed by adjusting the difference of the surface tension coefficients between the inner and outer surfaces. It is clear from equations (13) and (14) that in such cases the transition temperature also depends on the average radius R of the NTs as well as $\Delta\mu$. In figure 4, we plot the calculated transition temperature T_c as a function of the average radius R for different values of $\Delta\mu/\bar{\mu}$. It can be seen that positive values of $\Delta\mu/\bar{\mu}$ cause an increase of T_c, which increases as the average tube radius R decreases. The increase is most rapid for the small-radius tubes with an average tube radius of less than 10 nm. For a value of $\Delta\mu/\bar{\mu} = 30\%$, the T_c for a tube with an average radius of 2.5 nm can be higher by 100 K than one at 10 nm. For tube with radii larger than 25 nm, T_c is relatively insensitive to the tube size.

In addition to raising the transition temperature, the enhancement of ferroelectricity in NTs via the effects of the surface tension can also be seen directly from the strength of the average polarization. Solving equations (28) and (29), we obtain the average polarization for a BTO NT of inner radius $a = 10$ nm and surface energy density $\mu = 20$ N m^{-1} as a function of wall thickness w, which we plot in figure 5. The blue line shows similar results obtained without considering surface tension (i.e. $\mu = 0$ N m). The enhancement effect of the polarization due to the surface tension is obvious, and follows the same trend as the transition temperature, reaching a maximum near $w = 8$ nm, at which point the stress in the tube caused by the surface tension maximizes at the yield point. The results in figure 5 also demonstrate directly the existence of a critical wall thickness w_c of about 3.2 nm at 0 K, below which the polarization disappears. In figure 6, we show the corresponding plot of the polarization as a function of the average tube radius R for various values of $\Delta\mu$. The similarity between figures 4 and 6 is obvious.

Following Wang and Woo [18], we use a perturbation approach to solve equations (25) and (26), from which a Curie–Weiss-type relation of the dielectric permittivity can be obtained for a BTO NT with different wall thickness near the transition temperature (figure 7).

The results of figures 5–7 clearly show that the phase transition temperature, polarization and susceptibility are all controllable via various geometric factors of the NT. In

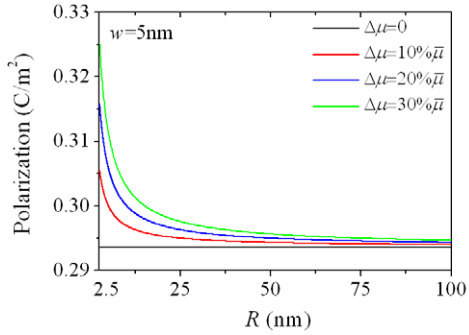

Figure 6. The polarization versus the average radius R, where the inner and outer surface tension coefficient is considered as a difference, such as $\Delta\mu = 10\%\bar{\mu}$, $20\%\bar{\mu}$ and $30\%\bar{\mu}$.

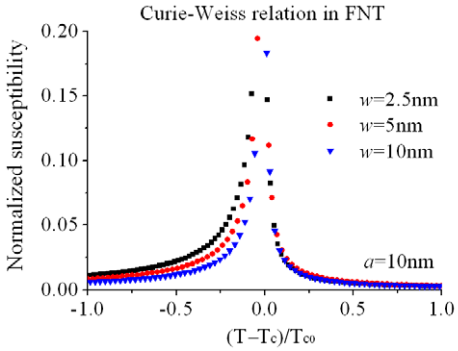

Figure 7. The Curie–Weiss-type relation in ferroelectric NTs, where the wall thickness is $w = 2.5$ nm, 5 nm and 10 nm, respectively.

evaluating the normalized susceptibility, $\Theta^{-1}(\delta, w)/(T - T_c)$, the transition temperature T_c is from result of figure 3. It can be seen that when the ferroelectric NT is in the paraelectric state ($T > T_c$) the Curie–Weiss relation is independent of the geometry of the tube. When the ferroelectric NT is in the ferroelectric state, the Curie–Weiss relation is a function of the wall thickness, radius and extrapolation length.

3.2. Polarization switching and hysteresis loops

Many experiments have shown results indicating the possible importance of the surface tension to the ferroelectric response

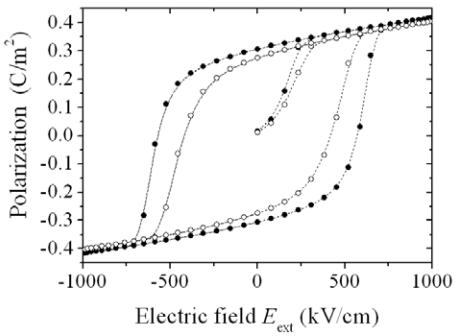

Figure 8. Hysteresis loops of the BTO NT at room temperature (the inner radius, outer radius and wall thickness are $a = 10$ nm, $b = 30$ nm and $w = 20$ nm, respectively), with and without surface tension effects, shown as filled and open cycles, respectively.

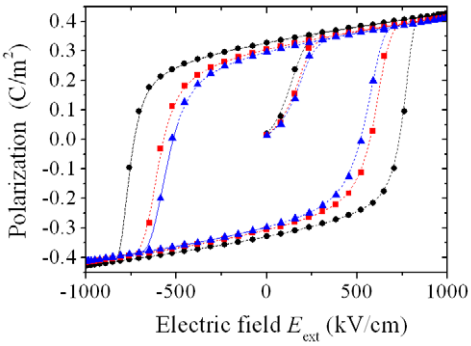

Figure 9. Hysteresis loops at room temperature for BTO NTs with varying wall thicknesses of $w = 10$ nm (solid cycle), 20 nm (solid square) and 30 nm (solid triangle), respectively, assuming $\Delta\mu = 0$.

of an NT when subjected to an external field, due to effects such as the enhancement of remnant polarization and the coercive field [1, 2]. To investigate such effects on polarization switching and hysteresis loops, we solve the TDGL equation (15) for the polarization response of a ferroelectric NT under a sinusoidal external electric field E_{ext} at room temperature and 300 K. The amplitude E_0 of the external field we used is $E_0 = 1000$ kV cm^{-1}. The time step is $\Delta t = T_p/N$ with $T_p = 3$ ns and the total number of time steps N within a period T_p is 5000. We use the finite-difference method for the spatial integration and the Runge–Kutta method for temporal integration to solve the TDGL equation in real space.

In the following, we consider the polarization switching behavior of the BTO NT. Note that the polarization considered here is the total polarization, that is, the sum of the self-polarization and the induced polarization. In figure 8, the resulting hysteresis loops for the BTO NT with and without surface tension effect are shown as filled and open cycles, respectively. For a surface energy density of $\mu = 20$ N m^{-1}, the hysteresis loop with the surface tension can be clearly traced by following the filled circles. The effect of the surface tension on both the remnant polarization and the coercive field in NT can be clearly seen as enhancements. The main reason for this enhancement is, as discussed, the electrostrictive effect of the stresses due to the surface tension. The behavior of hysteresis loops is consistent with experimental results of ferroelectric NTs in [1].

Figure 9 shows hysteresis loops at room temperature for BTO NTs with varying wall thicknesses of $w = 10$ nm (solid cycle), 20 nm (solid square) and 30 nm (solid triangle), respectively. The hysteresis loops can be seen to clearly depend on wall thickness of NTs. The remnant polarization and the coercive field can be seen to increase with decreasing thickness, consistent with the polarization enhancement due to surface tension.

4. Summary

In this paper, a thermodynamic model for the investigation of the properties of a ferroelectric NT is established. Based on linear stability analysis and numerical solution of the time-dependent Ginzburg–Landau evolution equation, the polarization, phase transition temperature, Curie–Weiss relation and hysteresis loops of the NT are calculated, and effects of the surface tension and the near-surface eigenstrain relaxation are investigated. Our results show that the two effects influence the ferroelectricity of the NT in opposite ways. The former tends to increase, while the latter to reduce, the ferroelectricity in the tube as its wall thickness decreases. As a result, the ferroelectric behavior of the NT depends on the details of how these two effects, which depend on material properties in different ways, are balanced. Elastic, as well as plastic, properties of the material are both found to be important. In addition to the material properties, geometric factors such as the wall thickness are found to be convenient design parameters. For the BTO NT considered here, the surface tension seems to be the stronger of the two surface effects, producing a general increase of the ferroelectric polarization in the NT above the bulk values as the wall thickness decreases. A similar behavior also applies to the remnant polarization and the coercive field of the hysteresis loop. Other effects such as those related to the electric boundary conditions and dislocation generation are out of our present scope, and have to be considered in further work.

Acknowledgments

This project was supported by grants from the Research Grants Council of the Hong Kong Special Administrative Region (5322/04E). Co-author BW is also grateful for support from the National Science Foundation of China (Nos 50232030, 10172030 and 10572155) and the Science Foundation of Guangzhou Province (2005A10602002) and Heilongjiang.

References

[1] Liu W, Sun X H, Han H W, Li M Y and Zhao X Z 2006 *Appl. Phys. Lett.* **89** 163122
[2] Alexe M, Hesse D, Schmidt V, Senz S, Fan H J, Zacharias M and Gosele U 2006 *Appl. Phys. Lett.* **89** 172907
[3] Jang J E, Cha S N, Amaratunga G A J, Kang D J, Hasko D G, Jung J E and Kim J M 2005 *Appl. Phys. Lett.* **87** 263103

[4] Luo Y, Szafraniak I, Zakharov N, Nagarajan V, Steinhart M, Wehrspohn R B, Wendorff J H, Ramesh R and Alexe M 2003 *Appl. Phys. Lett.* **83** 440
[5] Ma W H, Zhang M S and Lu Z H 1998 *Phys. Status. Solidi* b **166** 811
[6] Zhou Z H, Gao X S, Wang J, Fujihara K, Ramakrishna S and Nagarajan V 2007 *Appl. Phys. Lett.* **90** 052902
[7] Morrison F D, Luo Y, Szafraniak I, Nagarajan V, Wehrspohn R B, Steinhart M, Wendroff J H, Zakharov N D, Mishina E D, Vorotilov K A, Sigov A S, Nakabayashi S, Alexe M, Ramesh R and Scott J F 2003 *Rev. Adv. Mater. Sci.* **4** 114
[8] Naumov I I and Fu H X 2005 *Phys. Rev. Lett.* **95** 247602
[9] Zhong W L, Wang Y G, Zhang P L and Qu B D 1994 *Phys. Rev.* B **50** 698
[10] Huang H T, Sun C Q, Zhang T S and Hing P 2001 *Phys. Rev.* B **63** 184112
[11] Huang H T, Sun C Q and Hing P 2000 *J. Phys.: Condens. Matter* **12** L127
[12] Uchino K J, Sadanaga E J and Hirose T 1989 *J. Am. Ceram. Soc.* **72** 1555
[13] Morozovska A N, Eliseev E A and Glinchuk M D 2006 *Phys. Rev.* B **73** 214106
[14] Morozovskaya A N, Eliseev E A and Glinchuk M D 2006 *Physica* B **322** 356
[15] Wang B and Woo C H 2005 *J. Appl. Phys.* **97** 084109
[16] Woo C H and Zheng Y 2008 *Appl. Phys.* A **91** 59
[17] Zheng Y, Woo C H and Wang B 2008 *Acta Mater.* **56** 479
[18] Wang B and Woo C H 2006 *J. Appl. Phys.* **100** 044114
[19] Wang J and Zhang T Y 2006 *Phys. Rev.* B. **73** 144107
[20] Zheng Y, Wang B and Woo C H 2007 *J. Mech. Phys. Solids* **55** 1661
[21] Zheng Y, Wang B and Woo C H 2006 *Appl. Phys. Lett.* **88** 092903
[22] Pertsev N A, Zembilgotov A G and Tagantsev A K 1998 *Phys. Rev. Lett.* **80** 1988
[23] Hu S Y, Li Y L and Chen L Q 2003 *J. Appl. Phys.* **94** 2542
[24] Padilla J and Vanderbilt D 1997 *Phys. Rev.* B **56** 1625
[25] Ishikawa K J and Uemori T 1999 *Phys. Rev.* B **60** 11841
[26] Glinchuk M D and Morozovskaya A N 2003 *Phys. Status. Solidi* b **238** 81
[27] Timoshenko S P and Gooier J N 1970 *Theory of Elasticity* (New York: McGraw-Hill)
[28] Morozovska A N and Glinchuk M D 2006 *Preprint* cond-mat/0608595
[29] Morozovska A N, Glinchuk M D and Eliseev E A 2007 *Phase Trans.* **80** 1
[30] Dawber M, Rabe K W and Scott J F 2005 *Rev. Mod. Phys.* **77** 1083
[31] Li S P, Eastman J A, Li Z, Foster C M, Newnham R E and Cross L E 1996 *Phys. Lett.* A **212** 341
[32] Zheng Y, Wang B and Woo C H 2006 *Appl. Phys. Lett.* **89** 083115
[33] Zheng Y, Wang B and Woo C H 2006 *Appl. Phys. Lett.* **89** 062904
[34] Liu G and Nan C W 2005 *J. Phys. D: Appl. Phys.* **38** 584
[35] Glinchuk M D and Morozovska A N 2004 *J. Phys.: Condens. Matter* **16** 3517